J Sol-Gel Sci Technol (2012) 63:177–186
DOI 10.1007/s10971-012-2783-x

ORIGINAL PAPER

Controlling the growth of particle size and size distribution of silica nanoparticles by the thin film structure

Bengü Özuğur Uysal · Fatma Z. Tepehan

Received: 1 February 2012 / Accepted: 23 April 2012 / Published online: 5 May 2012

Abstract Nanostructured silicondioxide thin films were prepared by sol–gel spin coating technique. The SiO_2 films were made using a conventional mixture of tetraethoxysilane (TEOS), deionized water and ethanol with various NH_3/TEOS ratios. The nanostructured silica films were made using a mixture of the SiO_2 sol and regular SiO_2 sol to control the enlargement of the particles inside the films. The structural, morphological and optical characterizations of the as-deposited and annealed films were carried out using X-ray diffraction (XRD), atomic force microscopy, scanning electron microscopy, NKD spectrophotometer and ultraviolet–visible (UV–vis) spectroscopy. The transmittance data of the infrared spectra of the films were recorded using an FT-IR Spectrometer. The XRD studies showed that as-deposited films were amorphous and the formation of the alfa-cristobalite phase of the silica film was investigated at annealing temperature close to 1,100 °C. Optical properties of the transmittance spectra in the *s* and *p*-polarization modes were collected. Refractive indices and extinction coefficients were determined with respect to the NH_3/TEOS ratios in the compositions of the films. Optical cut-off wavelength values were investigated from the extrapolation of the absorbance spectra which was estimated from the UV–vis spectroscopy measurements. A red shift in the absorption threshold indicated that the size of silica nanoparticles was increased by an increase in the NH_3/TEOS volume ratio from 1:64 to 1:8.

Keywords Metaloxides · Nanoparticles · Sol–gel method · Particle size

1 Introduction

Nanostructured silicondioxide thin films and their composites with different metal oxides are important in various fields of nanotechnology. Solar cells, collector applications and optical filters [1, 2], catalyst and catalyst carriers [3], multilayered pyroelectric thin film detectors [4], the ceramic industry, lithium batteries [5, 6], thermochromics [7], gas sensors and bioanalytical applications [8, 9], fluoroesans pH sensors, humidity sensors [10], nanophotonics and microelectronics [11] are some examples of the application areas. Nanocomposite thin films show interesting mechanical, optical and electrical properties due to their size dependent character that differs from their bulk material. Several techniques [3, 10, 12–23] are available for the preparation of bulk, silica, nanostructured silica thin films and silica powder. Among these techniques, sol–gel is the most commonly used because of its simplicity and large area of applications. A large number of studies have been made on SiO_2 composite thin films using the sol–gel method [1, 2, 11, 24–26]. The optical properties and surface morphology of sol–gel spin coated WO_3 and WO_3–SiO_2 composite films have been investigated and were accurately modeled using a novel dielectric function consisting of two Tauc–Lorentz oscillators with an Urbach tail contribution [24]. SiO_2 together with TiO_2 and Ta_2O_5 thin films are used as optical filters [2] by the sol–gel spin coating method [25]. Other researchers have studied the

B. Ö. Uysal (✉)
Department of Information Technology, Faculty of Engineering and Natural Sciences, Kadir Has University, Cibali, Fatih, Istanbul 34083, Turkey
e-mail: bozugur@khas.edu.tr

B. Ö. Uysal · F. Z. Tepehan
Department of Physics Engineering, Faculty of Science and Letters, Istanbul Technical University, Maslak, Istanbul, Turkey

size-dependent structural and optical properties of silica nanoparticles highlighting the change in physicochemical properties of silica at smaller sizes and unique optical absorption characteristics [12–18]. The effect of the particle size with respect to the doping ratio of the SiO_2 sols have been investigated by some other researchers [19–23]. The size optimization of silica nanoparticles using statistical analyses was reported by Davies et.al. [27]. Controlling the particle size and size distribution is extremely important for the quality of the silica contained products [14].

In this study, we aimed to synthesize the silica and nanostructured silica films containing narrow size distributed nanoparticles. The effects of various NH_3/TEOS ratios on the particle size were investigated. In addition, the regular silica and silica sols were mixed to produce the nanostructured-SiO_2 films. As a result, we expect the regular SiO_2 gel encapsulate the SiO_2 nanoparticles to prevent their growth. Also, the optical properties and surface morphology of SiO_2 and nanostructured-SiO_2 films were studied.

2 Experiment

2.1 Film preparation

The starter SiO_2 solution was prepared using tetraethoxysilane (TEOS) solved in ethanol and mixed with deionized (DI) water for the hydrolysis reaction in a volume ratio of 1:1:0.67. Then hydrochloric acid (HCl) used as a catalyst, was added to the regular SiO_2 solution at room temperature, until it became homogeneous and transparent.

The SiO_2 sol was made using a conventional mixture of TEOS, deionized water and ethanol, with various NH_3 solution/TEOS ratios ranging from 1:8 to 1:64.

The regular SiO_2 and SiO_2 solutions were mixed at room temperature for 30 min. in a volume ratio of 1:10 to obtain nanostructured silica films.

Corning (2947) and silica glasses were used as substrates. The solutions were spin coated on the substrates at 1,000 rpm for 30 s. The final coatings on corning substrates were heated at 450 °C for 1 h. and on silica substrates were heat treated at 1,100 °C for 36 h. by a microprocessor-controlled (CWF 1100) furnace.

2.2 Film characterization

After heat treatment, atomic force microscope (AFM; SPM-9500, Shimadzu Corp.) and scanning electron microscope (SEM; JSM-7000F, Jeol Ltd.) were used to study the detailed morphological surface analysis and nanostructure of the thin films. The transmittance data of the films were carried out by a spectrophotometer (NKD 7000, Aquila Inst.) in the *s* and *p* polarization modes in between 300 and 1,000 nm wavelength. Refractive indices and extinction coefficients were evaluated by the Pro-Optix software incorporated with this device. The thickness of the films was calculated using a Stylus Profilometer (Veeco, Dektak 150). The absorbance spectra of silica and nanostructured silica films were measured by UV–visible Spectrophotometer (Agilent 8453) in between 200 and 1,000 nm wavelength. Fluorescence properties of the nanostructured silica films was studied by Perkin-Elmer Model LS-50 Spectrometer, excited with the wavelength of 242 nm at room temperature. The Fourier transform infrared (FT-IR) spectra of the films in the transmission mode were recorded in a wave number range of 650–4,000 cm^{-1} on a Perkin-Elmer Spectrum FT-IR Spectrometer. The structure of the silica films was characterized by an X-Ray Diffractometer (GBC-MMA) using monochromatized Cu-Kα radiation ($\lambda = 1.54056$ Å). The XRD spectra of the films were recorded by scanning 2θ in the range 20°–80°, with a grazing angle of 1°.

3 Results and discussion

3.1 XRD analysis

The XRD analysis showed that the films were amorphous at the heat treatment temperature of 450 °C. For regular SiO_2 film annealed at 1,100 °C (Fig. 1), no diffraction peak was observed except for a broad band centered at $2\theta = 22.00°$, which is the characteristic behavior for amorphous SiO_2 (JCPDS 29-0085). On the other hand, a very strong crystallization of the α-SiO_2 (α-cristobalite phase) at $2\theta = 22.08°$ and 36.10°, occurred for the silica films at the annealing temperature of 1,100 °C. Previously, similar α-cristobalite structure was observed at 1,100 °C [23, 28].

The average crystallite size was determined from the Scherrer's equation below:

$$D = \frac{K\lambda}{B\cos\theta},$$

where D is the diameter of the silica nanocrystals, K is a constant (0.89), λ is the wavelength of the incident light (for Cu Kα radiation $\lambda = 1.54056$ Å), B is the full width at half-maximum (FWHM) of the diffraction line and θ is the Bragg angle. The nanocrystallite sizes are found to be 8.9, 12.1 and 33.8 nm for SiO_2 thin film with ratios of NH_3/TEOS = 1:64, 1:32, 1:16, respectively. The weakening and broadening of the XRD peaks could be attributed to the decrease of the crystallite size. The particle size of silica films was reduced by a decrease in the NH_3/TEOS mole

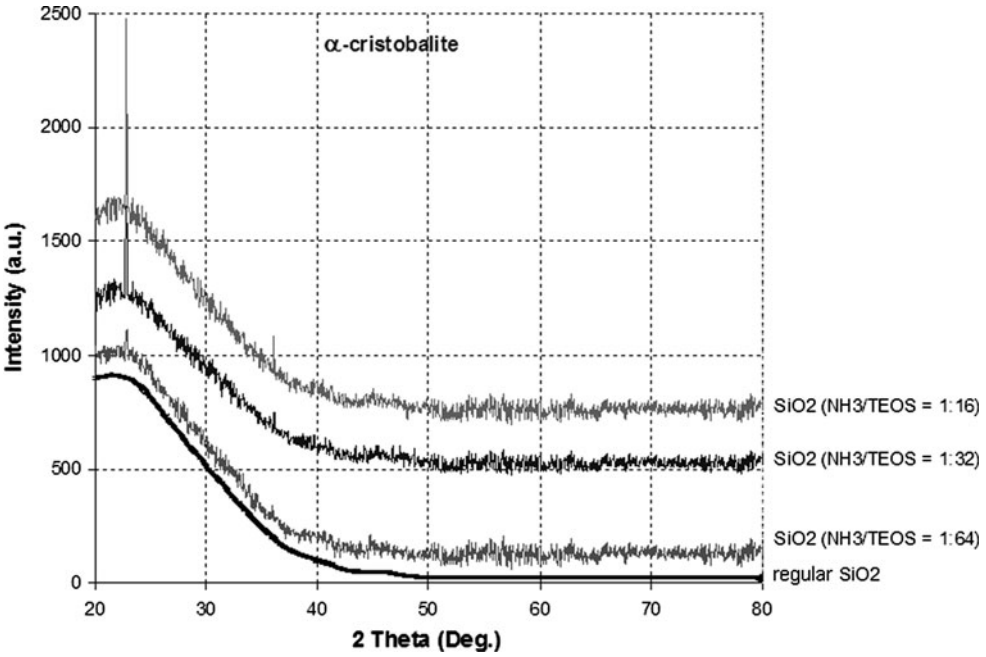

Fig. 1 XRD spectra of regular silicondioxide and silicondioxide films with different particle size annealed at 1,100 °C. The weakening and broadening of the XRD peaks could be attributed to the decrease of the crystallite size

ratio in the compositions. This result is consistent with the literature [12–18].

3.2 Surface morphology of the films

AFM images of the regular SiO_2 and SiO_2 films at the annealing temperature of 450 °C are given in Fig. 2a and b, respectively. In comparison with the regular SiO_2 film, the SiO_2 thin film manifested a granular structure. Fig. 2b and c show that a change in the NH_3/TEOS ratio in the solution of the film affects the size of the nanoparticles. The particle size of the silica thin films with the different ratio 1:32, 1:16, and 1:8 of NH_3/TEOS are observed approximately at 50, 80 and 110 nm from the AFM images as shown in Fig. 2 (b). On the other hand the nanostructured silica films synthesized with the mixture of regular SiO_2 and SiO_2 solutions in volume ratio of 1:10. According to the surface images of the nanostructured silica films, the greater the NH_3/TEOS ratio in compositions, the larger the nanoparticles as illustrated in Fig. 2(c). This result is in agreement with Stöber et. al. [29]. The maximum diameter of particles versus the number of particle distributions of the different SiO_2 films are presented in Fig. 3. Gaussian-like particle distributions centered about the mean particle size of the films shifted to a smaller particle diameter when the NH_3/TEOS ratio in compositions is decreased. However, particle sizes smaller than 10 nm could not be observed from the AFM. SEM measurements provided further nanoparticle observations. In the nanostructured silica films, the sizes of the silica nanoparticles, calculated by using the SPM Manager Program, are found to be about 16; 34; 59 nm by varying the NH_3/TEOS ratio of the sol from 1:32 to 1:8 as shown in Table 1, respectively. This ratio is inversely proportional to the number of particles per micrometer squares. On the other hand, when the ratio of NH_3/TEOS in compositions is decreased, the particles contained in the film displayed a more regular structure, and are aligned.

Figure 4 shows the FE-SEM surface micrograph of the nanostructured silica film (NH_3/TEOS = 1:64) which is formed by a SiO_2 structure consisting of the spherical nanostructured SiO_2 particles with an average size of 10 nm. These particles are non-aggregated and dispersed uniformly in the regular SiO_2 thin film. A cross-sectional SEM image of this film is shown in Fig. 5. The particles have a tubular-like alignment. The particle size is relatively smaller when compared with the envisaged values of average diameters from the particle distributions of the other films displayed in Fig. 3.

Table 2 shows the crystallite size of the SiO_2 and nanostructured-SiO_2 thin films with respect to the varying ratio of NH_3/TEOS in compositions at annealing temperature of 450 °C. In addition Table 2 also shows the size variation of SiO_2 films with respect to the same ratios of NH_3/TEOS heat treated at 1,100 °C. It is clearly seen that the particle size of all films grows when the ratio of NH_3/TEOS increases. Comparison of the SiO_2 and nanostructured-SiO_2 thin film heat treated at 450 °C show that the size of the nanostructured-SiO_2 films are smaller at each ratios of NH_3/TEOS. The growth of the silica nanoparticles is prevented by this structure. Because the nanoparticles are encapsulated by the regular SiO_2 gel. The size of the nanoparticles of SiO_2 films decreased when they are heat treated at 1,100 °C with respect to the films heat treated at

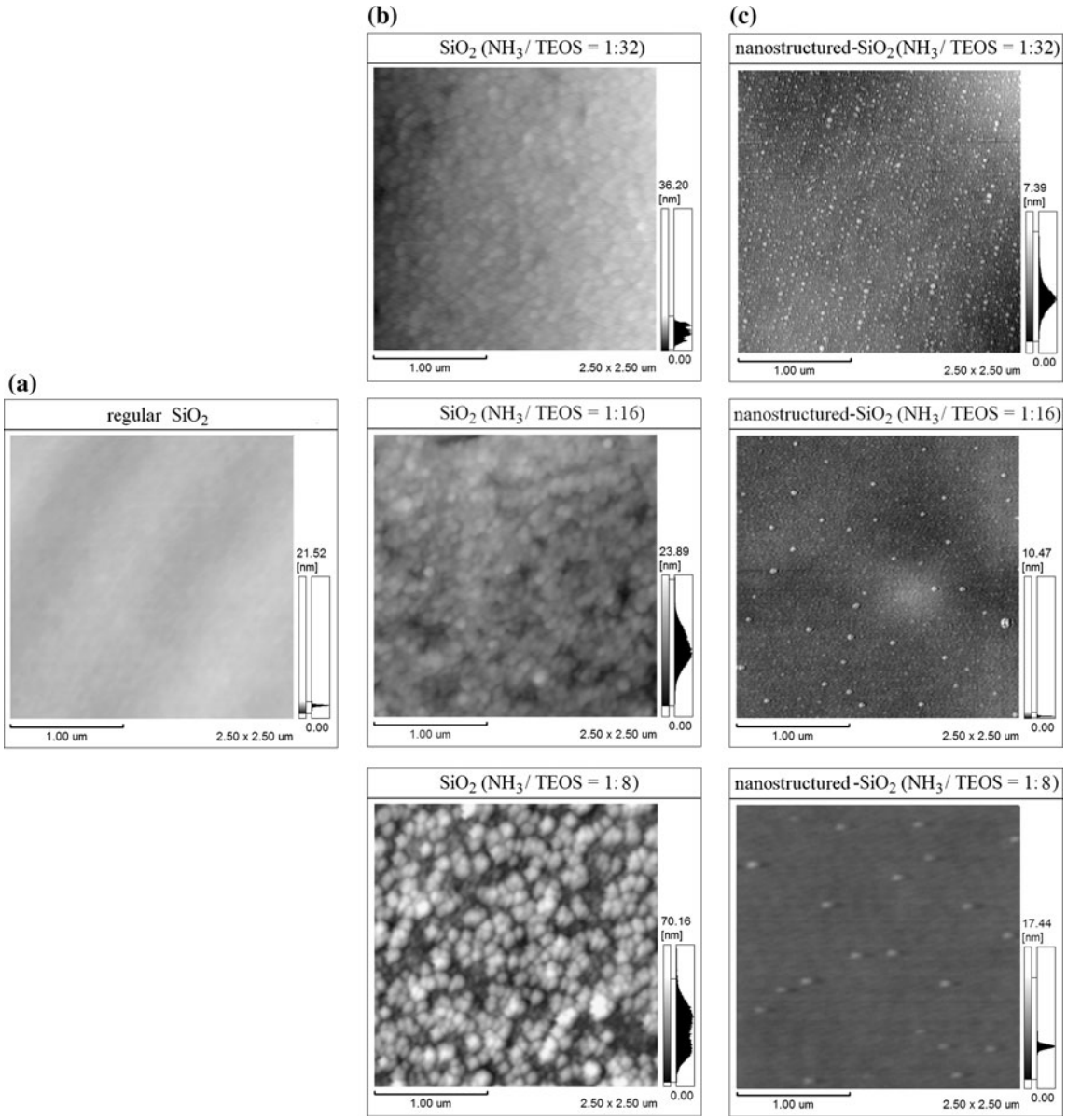

Fig. 2 AFM images of **a** regular SiO_2 film, **b** SiO_2 film and **c** nanostructured SiO_2 particles with different NH_3/TEOS ratios in regular SiO_2 thin film

450 °C. It is clear from the XRD measurements, the amorphous phase of the silica thin film was transformed into the alfa-cristobalite phase when heat treated at 1,100 °C.

The Fourier transform infrared (FT-IR) spectra of the films in the transmission mode are recorded in the wave number range of 650–4,000 cm^{-1} as presented in Figs. 6 and 7. The transmission bands of Si–O–Si (asymmetric stretching, 1,029-1,059 cm^{-1}), Si–OH (symmetric stretching, ~930 cm^{-1}), and Si–O (bending, 799–768 cm^{-1}) bonds are observed for the SiO_2 film in Fig. 6. The Si–O-Si stretching motion, which was expected [30–32] to be about 1,080 cm^{-1}, shifted to lower wavenumber values with the decrease of the size of the silica nanoparticles. Figure 7 shows the FT-IR spectra of nanostructured silica films which exhibit similar behavior of FT-IR spectra of the SiO_2 films as seen in Fig. 6. The Si–O-Si asymmetric stretching vibration shift to higher wavenumbers was observed by other groups [32–34] as the heat treatment temperature is increased. The transverse optical (TO) component of the asymmetric stretching vibration of Si–O–Si bond shifted to the lower wavenumber values (from 1,049 to 1,020 cm^{-1}) when particle size of the films decreased. Chemically, the decrease in amount of the catalyzer material (in this case NH_3 solution) effects the particle distribution in the solution, and it leads to the coagulation in the clustered

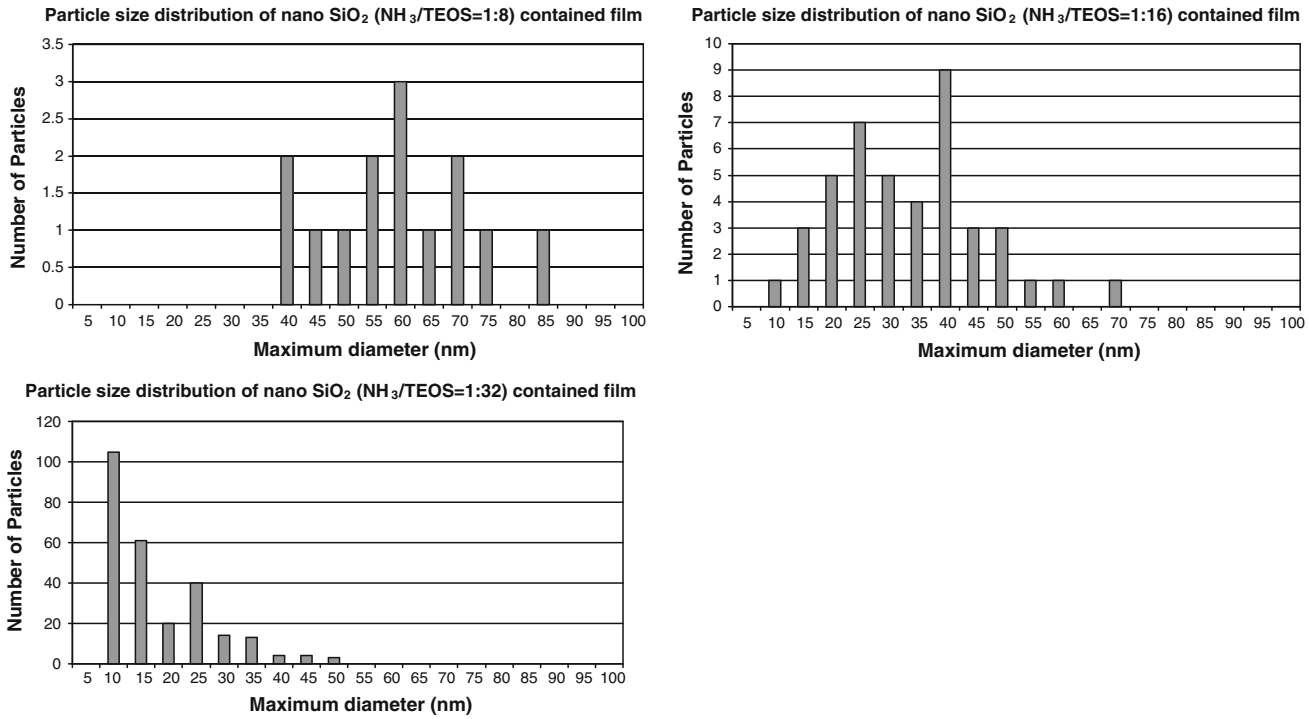

Fig. 3 Particle size distributions of SiO_2 nanoparticles with different NH_3/TEOS ratios in regular SiO_2 thin film with SPM Manager Program

Table 1 Profile analysis results of nanostructured silicondioxide thin films with different ratio of NH_3/TEOS

Ratio of NH_3/TEOS	Maximum particle diameter (nm)	Surface area (nm^2)	Number of particles per 2.5 × 2.5 nm^2
1/32	16	50,541	252
1/16	34	39,779	49
1/8	59	38,640	14

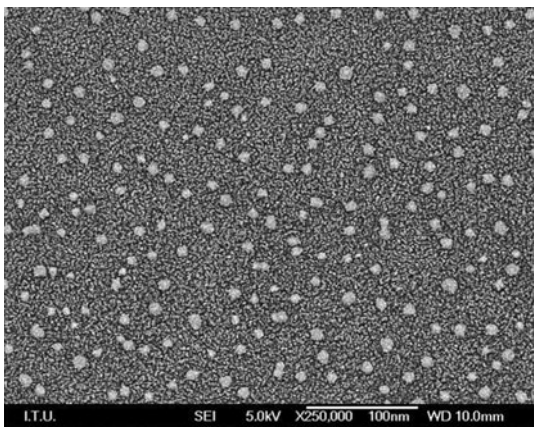

Fig. 4 FE-SEM image of the nanostructured silica film (NH_3/TEOS = 1:64). Silica nanoparticles are non-aggregated and dispersed uniformly in the regular SiO_2 thin film

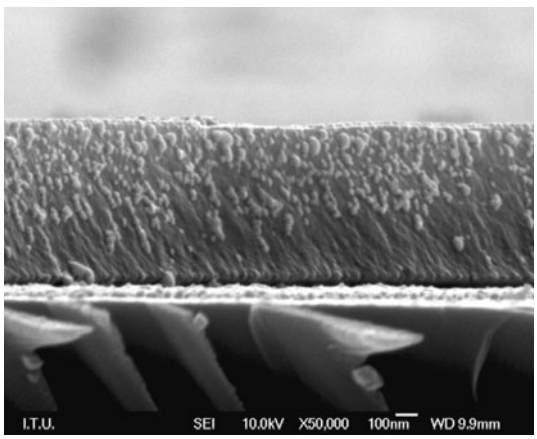

Fig. 5 Cross-sectional FE-SEM image of the nanostructured-SiO_2 film to illustrate the alignment of nanoparticles

medium. The possible reason is that owing to the effect of finite size of nanoparticles, the bonds of surface atoms are breaking. Therefore, the inlocalized electrons on the surface of particles are rearranged and the lattice constrictions [35] like change in symmetry occur. Meanwhile, the lower wavenumbers which correspond to lower frequencies may caused by the cross-linking of the Si–O–Si chains while the synthesized particles are smaller due to the decreasing ratio

Table 2 Particle sizes (nm.) of the silica and nanostructured silica thin films

Ratio of NH_3/TEOS	Calculated by SPM Manager and SEM nanostructured SiO_2 film at 450 °C	Observed with AFM SiO_2 film at 450 °C	Calculated by Scherrer equation with XRD data SiO_2 film at 1,100 °C
1:64	10	–	8.9
1:32	16	50	12.1
1:16	34	80	33.8
1:8	59	110	–

of NH_3/TEOS in compositions. All that leads to the shifting of the transmission bands of FT-IR spectrum to the lower wavenumbers as reported before [32, 34].

3.3 Optical properties

Figures 8 and 9 show the transmittance spectra of the silica and nanostructured silica films respectively in a spectral range of 300–1,000 nm at an incidence angle of 30° for *s* and *p*-polarization modes. Decreasing the ratio of NH_3/TEOS in composition increased the transmittance for both *s* and *p* polarization modes. The transmittance of the SiO_2 films changed from 67 to 73 % in the *s*-polarization mode and from 70 to 77 % in the *p*-polarization mode at 550 nm with the decrease of the NH_3/TEOS ratio from 1:8 to 1:64. Higher transmittance observed in the ratio of 1:64 is attributed to the structural homogeneity and the smaller size of the nanoparticles in the silica films. Figure 9 shows that the transmittance of the nanostructured-SiO_2 films changed from 85 to 89 % in the *s*-polarization mode and from 87 to 92 % in the *p*-polarization mode at 550 nm with the decrease of the NH_3/TEOS ratio. Higher transparence ratio for the nanostructured-SiO_2 film is due to the smaller concentration of silica nanoparticles.

Refractive indices and the extinction coefficients of the films are calculated by Pro-optix software as a function of wavelength. In Fig. 10, the refractive index of the nanostructured-SiO_2 films decreases from 1.58 to 1.53 with the

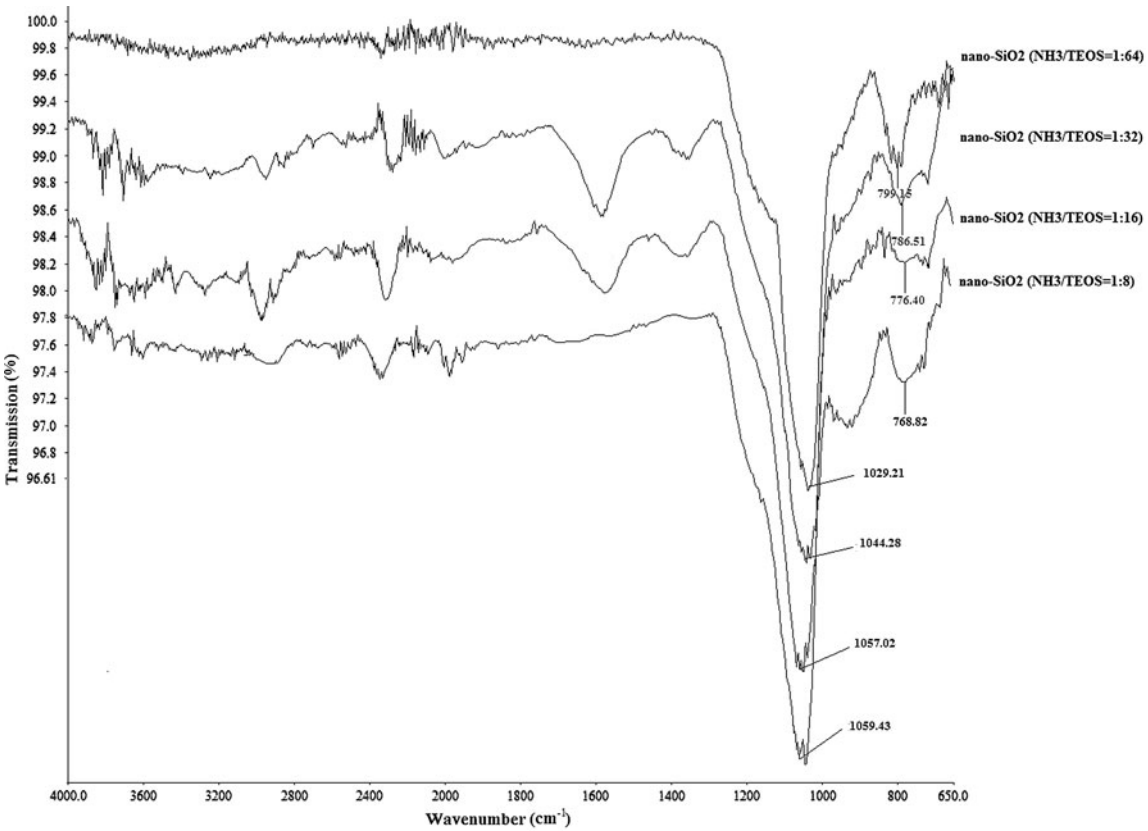

Fig. 6 FT-IR spectra of the SiO_2 films have different sized nanoparticles

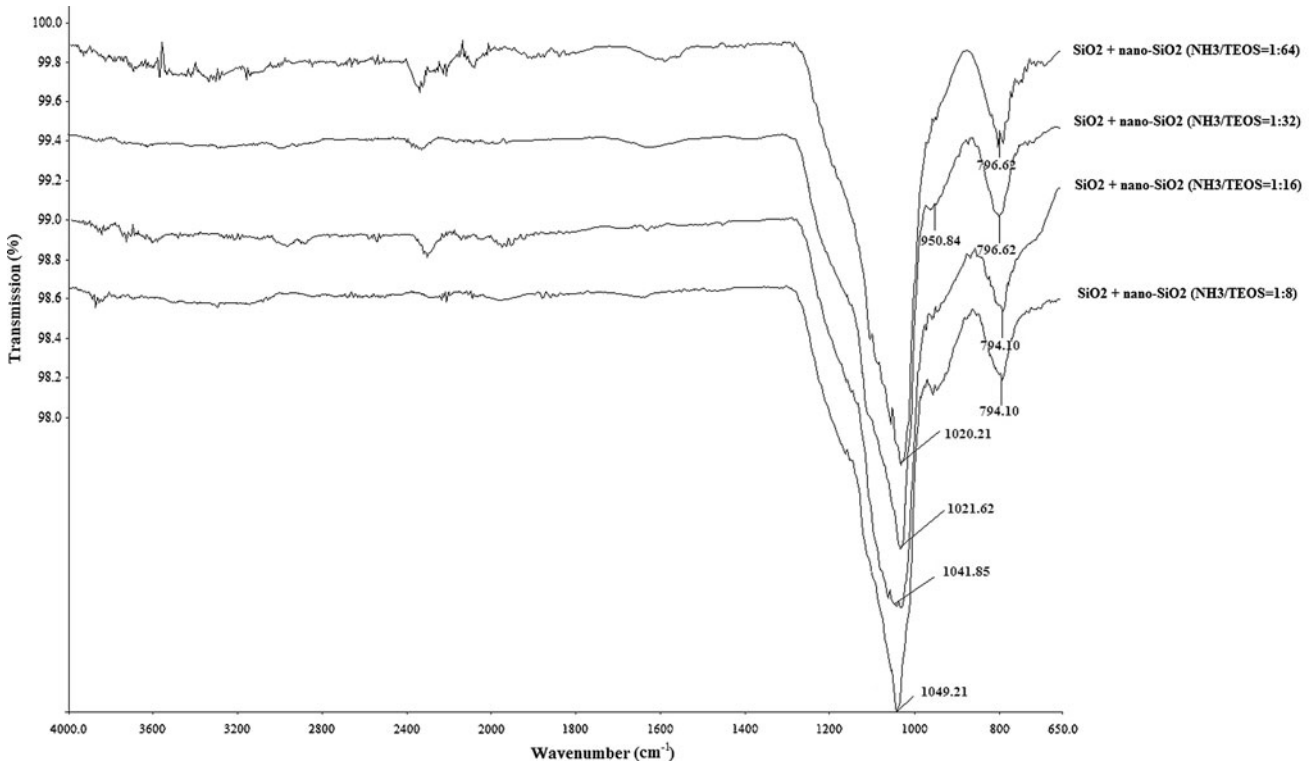

Fig. 7 FT-IR spectra of the nanostructured-SiO_2 films with different NH_3/TEOS ratios

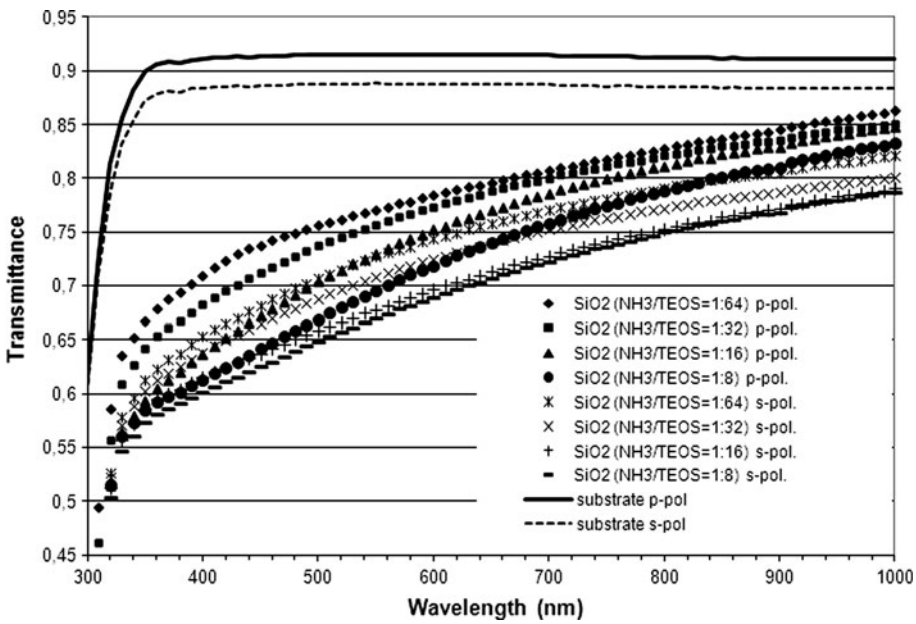

Fig. 8 Transmittance data of SiO_2 films with respect to the wavelength of different NH_3/TEOS ratios

decrease of the NH_3/TEOS ratio in the sols from 1:8 to 1:64 at 550 nm. The extinction coefficients of all nanostructured silica films with different ratios of NH_3/TEOS have minimum at the wavelength of 350 nm as seen in Fig. 11. The transmittance of the film is very high at longer wavelengths, because the distance between the nanoparticles is big enough to transmit the light. The thickness of the film allows to the incident light both absorbs and transmits in the film.

The absorbance spectra of nanostructured silica films were measured with a UV–vis spectrophotometer, as seen in Figs. 12 and 13. Extrapolation of the absorbance spectra

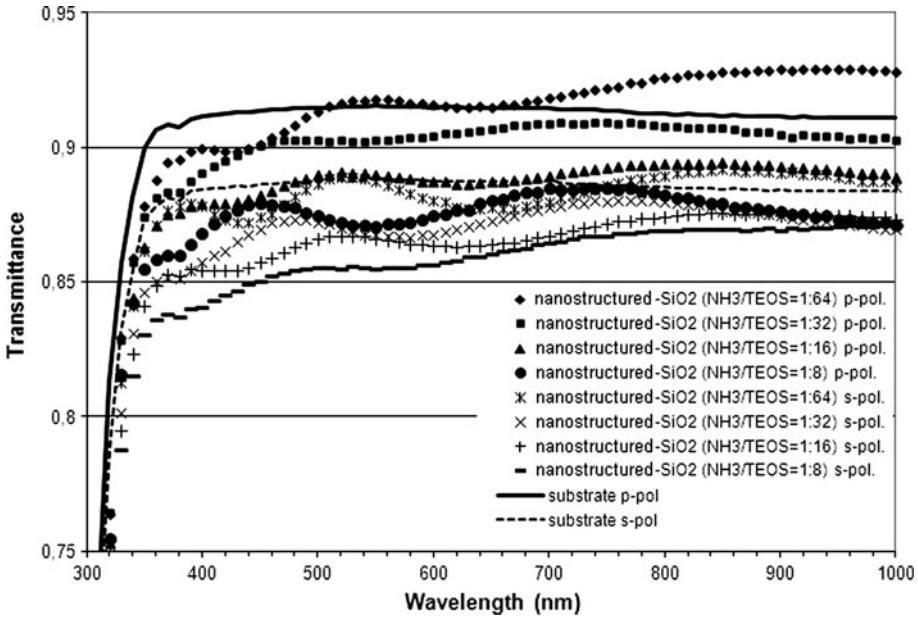

Fig. 9 Transmittance data of nanostructured -SiO_2 film with different NH_3/TEOS ratios

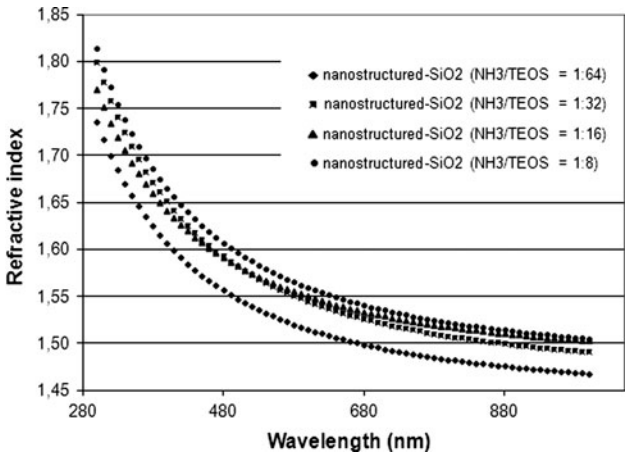

Fig. 10 Refractive indices of the nanostructured silica thin films have different particle sizes

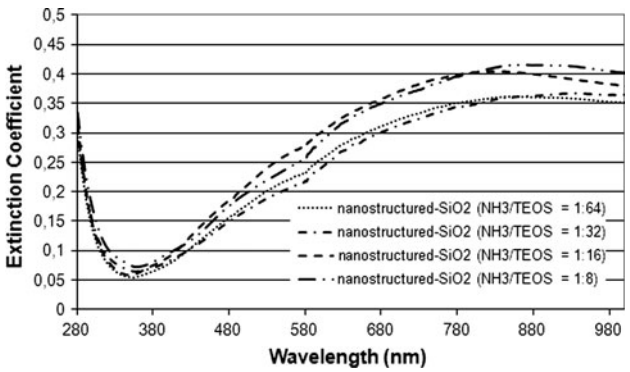

Fig. 11 Extinction coefficients of the nanostructured silica thin films

gives the information about the cut-off wavelength of the films. The cut-off wavelength of the absorption edge shifted to longer wavelengths (red–shifted) with increasing particle size, as seen in Figs. 12 and 13. As is very well known, the absorption coefficient, α is proportional to the extinction coefficient, κ ($\alpha = 4\pi\kappa/\lambda$). Both absorbance and extinction coefficients data are proved the equation.

Figure 14 shows the fluorescence spectra of nanostructured silica films at different NH_3/TEOS ratios in compositions excited with a 242 nm light. The position of maximum emission peak is shifted to the higher wavelength (red shifted) as the NH_3/TEOS ratio increase. The other maxima of the fluorescence spectra are attributed to the vibrational effect of the energy levels of the solid state. Figure 14 also shows that the intensity increased with the decrease of NH_3/TEOS ratios in composition. The shifts in the fluorescence emission maxima values in Fig. 14 are

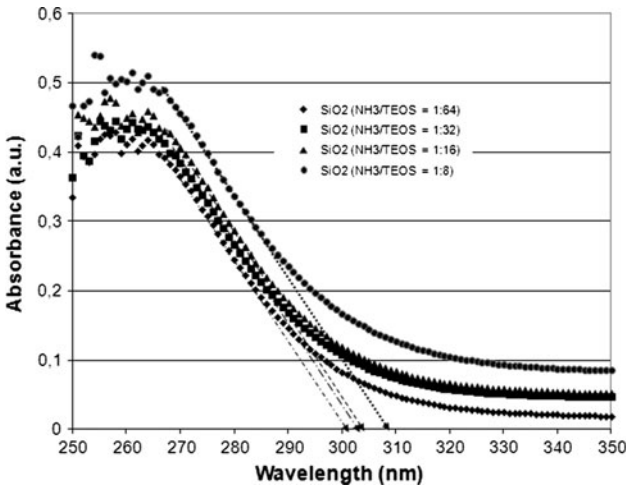

Fig. 12 UV–vis absorbance spectra of silicondioxide films with different particle size

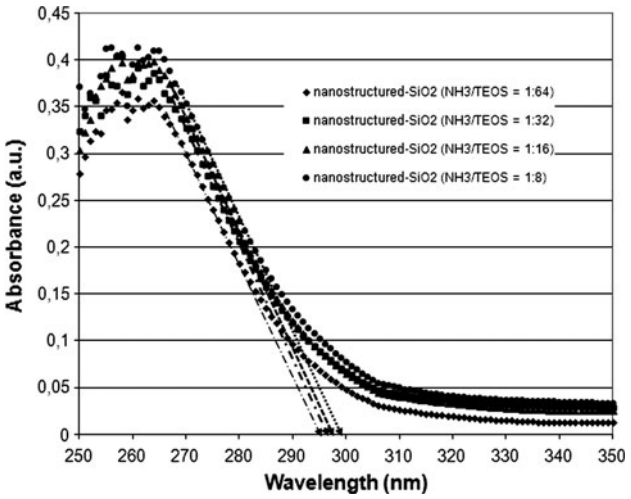

Fig. 13 Extrapolation of the UV–vis absorbance spectra of nanostructured silicondioxide films with different particle size

compatible with the shifts in the cut-off wavelength values of the nanostructured-SiO_2 films.

4 Conclusion

The present study has shown that the size of silica nanoparticles was reduced by a decrease in the NH_3/TEOS mole ratio of the films. SiO_2 nanoparticles embedded in the regular SiO_2 thin films have controlled the size of the particles inside the films. AFM measurements and experimental results showed that SiO_2 nanoparticles were distributed almost uniformly in the regular SiO_2 thin film matrix at the annealing temperature of 450 °C. The nanoparticles are encapsulated by the regular SiO_2 gel and therefore the nanostructured silica film has smaller particles than the silica film with the same ratio of NH_3/TEOS at the same annealing temperature. As a result, the growth of the silica nanoparticles is prevented by this structure.

The amorphous phase of the silica thin film was transformed into the alfa-cristobalite phase due to the heat treatment which occurred at 1,100 °C. The weakening and broadening of the XRD peaks were attributed to the decrease of the crystallite size due to the reduced NH_3/TEOS ratio in the compositions, which is consistent with the literature [12–18]. The optical studies revealed that the transmittance of the films increased and stabilized by doping nanoparticles in the sol. The higher transmittance observed in the ratio of 1:64 can be attributed to the structural homogeneity. The refractive index of the nanostructured-SiO_2 films decreases with a decrease in the NH_3/TEOS ratio. The absorption edge of the nanostructured films shifted to the longer wavelengths with the increasing ratio of NH_3/TEOS in compositions. The quantum confinement effect of nanoparticles was confirmed by the cut-off wavelength shift with both UV–vis and fluorescence measurements. The decrease of the calculated crystallite sizes of the thin films at the annealing temperature of 1,100 °C are also in agreement with the AFM and SEM measurements at 450 °C. In this study, the different particle sized silica films was added into the regular silica films, therefore it is possible to change the refractive index and the cut-off wavelength—also band gap energy—of the films, and this is crucial for the optical filter applications.

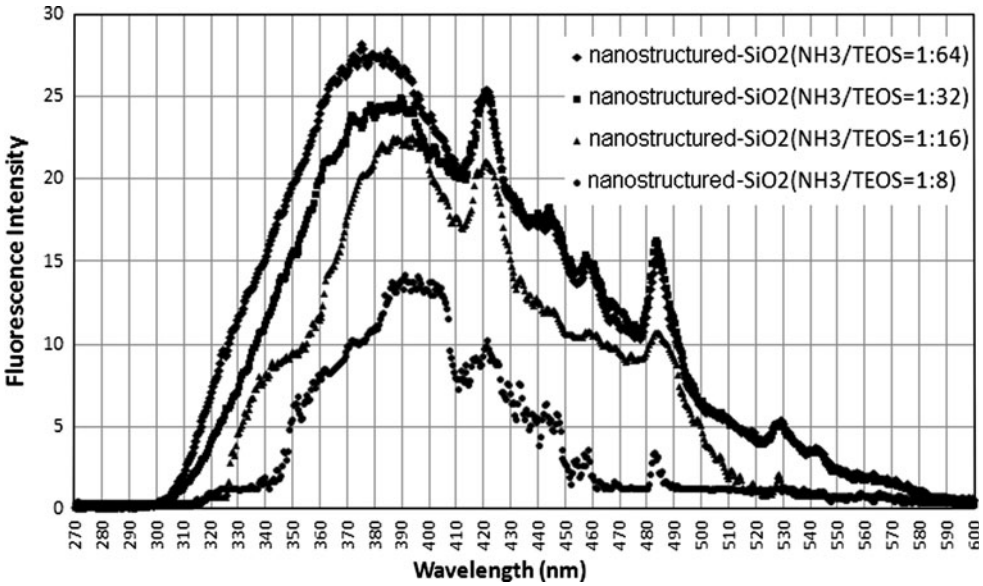

Fig. 14 Fluorescence spectrum of the nanostructured silica thin films

Acknowledgments The Research Fund of Istanbul Technical University has generously supported this research, and the authors would like to thank Prof. Dr. M. Urgen, Prof. Dr. G. Goller, and Prof. Dr. A. Gul for the SEM and FTIR measurements.

References

1. Schuler A, Dutta D, de Chambrier E, Roecker C, De Temmerman G, Oelhafen P, Scartezzini J-L (2006) Sol–gel deposition and optical characterization of multilayered $SiO_2/Ti_{1-x}Si_xO_2$ coatings on solar collector glasses. Sol Energy Mater Sol Cells 90:2894–2907
2. Saygın Hinczewski D, Hinczewski M, Tepehan FZ, Tepehan GG (2005) Optical filters from SiO_2 and TiO_2 multi-layers using sol–gel spin coating method. Sol Energy Mater Sol Cells 87:181–196
3. Duhan S, Devi S, Singh M (2009) Structural characterization of Nd doped in silica host matrix prepared by wet chemical process. J Rare Earths 27(1):83–86
4. Li L, Zhang L, Yao X (2004) Preparation and characterization of thick porous SiO_2 film for multilayer pyroelectric thin film IR detector. Ceram Int 30:1843–1846
5. Wang X-L, Cai Q, Fan L-Z, Hua T, Lin Y-H, Nan C-W (2008) Gel-based composite polymer electrolytes with novel hierarchical mesoporous silica network for lithium batteries. Electrochim Acta 53:8001–8007
6. Arumugam D, Paruthimal Kalaignan G (2008) Synthesis and electrochemical characterizations of Nano-SiO_2-coated $LiMn_2O_4$ cathode materials for rechargeable lithium batteries. J Electroanal Chem 624:197–204
7. Suzuki H, Yamaguchi K, Miyazaki H (2007) Fabrication of thermochromic composite using monodispersed VO_2 coated SiO_2 nanoparticles prepared by modified chemical solution deposition. Compos Sci Technol 67:3487–3490
8. Yao N, Cao S, Yeung KL (2009) Mesoporous TiO_2–SiO_2 aerogels with hierarchal pore structures. Microporous Mesoporous Mater 117:570–579
9. Vogel R, Surawski PPT, Littleton BN, Miller CR, Lawrie GA, Battersby BJ, Trau M (2007) Fluorescent organosilica micro- and nano-particles with controllable size. J Colloid Interface Sci 310:144–150
10. Wang C-T, Wu C-L, Chen I-C, Huang Y-H (2005) Humidity sensors based on silica nanoparticle aerogel thin films. Sens Actuators B 107:402–410
11. Vasiliu I, Gartner M, Anastasescu M, Todan L, Predoană L, Elişa M, Negrilă C, Ungureanu F, Logofătu C, Moldovan A, Bîrjega R, Zaharescu M (2007) Structural and optical properties of the SiO_2–P_2O_5 films obtained by sol–gel method. Thin Solid Films 515(16):6601–6605
12. Gurav JL, Nadargi DY, Rao AV (2008) Effect of mixed catalysts system on TEOS-based silica aerogels dried at ambient pressure. Appl Surf Sci 255:3019–3027
13. Huang Y, Pemberton JE (2010) Fabrication of colloidal arrays by self-assembly of sub-100 nm silica particles. Colloids Surf A Physicochem Eng Asp 360:175–183
14. Park SK, Kim KD, Kim HT (2002) Preparation of silica nanoparticles: determination of the optimal synthesis conditions for small and uniform particles. Colloids Surf A Physicochem Eng Asp 197:7–17
15. Marini M, Pourabbas B, Pilati F, Fabbri P (2008) Functionally modified core-shell silica nanoparticles by one-pot synthesis. Colloids Surf A Physicochem Eng Asp 317:473–481
16. Bae GY, Min BG, Jeong YG, Lee SC, Jang JH, Koo GH (2009) Superhydrophobicity of cotton fabrics treated with silica nanoparticles and water-repellent agent. J Colloid Interface Sci 337:170–175
17. Hou A, Yu Y, Chen H (2010) Uniform dispersion of silica nanoparticles on dyed cellulose surface by sol–gel method. Carbohydr Polym 79:578–583
18. Aubert T, Grasset F, Mornet S, Duguet E, Cador O, Cordier S, Molard Y, Demange V, Mortier M, Haneda H (2010) Functional silica nanoparticles synthesized by water-in-oil microemulsion processes. J Colloid Interface Sci 341:201–208
19. Hu X, Song Z, Wang H, Liu W, Zhang Z (2010) Investigation on the controllable growth of monodisperse silica colloid abrasives for the chemical mechanical polishing application. Microelectron Eng 87:1751–1755
20. Blute I, Pugh RJ, van de Pas J, Callaghan Ian (2009) Industrial manufactured silica nanoparticle sols. 2: surface tension, particle concentration, foam generation and stability. Colloids Surf A Physicochem Eng Asp 337:127–135
21. Blute I, Pugh RJ, van de Pas J, Callaghan I (2007) Silica nanoparticle sols 1. Surface chemical characterization and evaluation of the foam generation (foamability). J Colloid Interface Sci 313:645–655
22. Du H, Hamilton PD, Reilly MA, d'Avignon A, Biswas P, Ravi N (2009) A facile synthesis of highly water-soluble, core-shell organo-silica nanoparticles with controllable size via sol-gel process. J Colloid Interface Sci 340:202–208
23. Li X, Yin X, Zhang L, He S (2008) The devitrification kinetics of silica powder heat-treated in different conditions. J Non-Cryst Solids 354:3254–3259
24. Saygın Hinczewski D, Hinczewski M, Sorar İ, Tepehan FZ, Tepehan GG (2008) Modeling the optical properties of WO_3 and WO_3–SiO_2 thin films. Sol Energy Mater Sol Cells 92:821–829
25. Koc K, Tepehan FZ, Tepehan GG (2005) Antireflecting coating from Ta_2O_5 and SiO_2 multilayer films. J Mater Sci 40:1363–1366
26. Sorar I, Saygin-Hinczewski D, Hinczewski M, Tepehan FZ (2011) Optical and structural properties of Si-doped ZnO thin films. Appl Surf Sci 257:7343–7349
27. Davies G-L, Barry A, Gunko YK (2009) Preparation and size optimisation of silica nanoparticles using statistical analyses. Chem Phys Lett 468:239–244
28. Battisha IK, Afify HH, Badr Y (2002) Structural and photoluminescence behaviors of nano-structure thin film and bulk silica gel derived glasses. J Sol–Gel Sci Technol 25:5–15
29. Stöber W, Fink A, Bohn E (1968) Controlled growth of monodisperse silica spheres in the micron size range. J Colloid Interface Sci 26:62–69
30. El Rassy H, Pierre AC (2005) NMR and IR spectroscopy of silica aerogels with different hydrophobic characteristics. J Non-Cryst Solids 351:1603–1610
31. Rosero-Navarro NC, Figiel P, Jedrzejewski R, Biedunkiewicz A, Castro Y, Aparicio M, Pellice SA, Dura′n A (2010) Influence of cerium concentration on the structure and properties of silica-methacrylate sol–gel coatings. J Sol–Gel Sci Technol 54:301–311
32. Yi LX, Heitmann J, Scholz R, Zacharias M (2003) Phase separation of thin SiO layers in amorphous SiO/SiO_2 superlattices during annealing. J Phys Condens Matter 15:2887–2895
33. Yang H-S, Choi S-Y, Hyun S-H, Park H–H, Hon J-K (1997) Ambient-dried low dielectric SiO_2 aerogel thin film. J Non-Cryst Solids 221:151–156
34. Mehner A, Dong J, Prenzel T, Datchary W, Lucca DA (2010) Mechanical and chemical properties of thick hybrid sol–gel silica coatings from acid and base catalyzed sols. J Sol-Gel Sci Technol 54:355–362
35. Ma M, Zhang Y, Yu W, Shen H, Zhang H, Gu N (2003) Preparation and characterization of magnetite nanoparticles coated by amino silane. Colloids Surf A Physicochem Eng Asp 212: 219–226